Contrasting Mechanical Anisotropies of the Superfluid ^{3}He Phases in Aerogel

D. I. Bradley,[1] S. N. Fisher,[1] A. M. Guénault,[1] R. P. Haley,[1] N. Mulders,[2] S. O'Sullivan,[1] G. R. Pickett,[1] J. Roberts,[1] and V. Tsepelin[1]

[1]Department of Physics, Lancaster University, Lancaster, LA1 4YB, United Kingdom
[2]Department of Physics and Astronomy, University of Delaware, Newark, Delaware, USA
(Received 18 October 2006; published 14 February 2007)

There has been much recent interest in how impurity scattering may affect the phases of the *p*-wave superfluid ^{3}He. Impurities may be added to the otherwise absolutely pure superfluid by immersing it in aerogel. Some predictions suggest that impurity scattering may destroy orientational order and force all of the superfluid phases to have an isotropic superfluid density. In contrast to this, we present experimental data showing that the response of the *A*-like phase to superfluid flow is highly anisotropic, revealing a texture that is easily modified by flow.

DOI: 10.1103/PhysRevLett.98.075302 PACS numbers: 67.57.Pq, 67.57.De, 67.57.Fg, 67.57.Hi

Superfluid ^{3}He is intrinsically pure since the only solute, ^{4}He, has *zero* solubility at milliKelvin temperatures and, along with all other atomic impurities, freezes out on the cell walls. The pure bulk superfluid is well understood, the two common phases being the pseudoisotropic *B* phase, well-described by the Balian-Werthamer (BW) state [1], and the anisotropic *A* phase described by the Anderson-Brinkman-Morel (ABM) state [2,3]. However, there has been much recent controversy on the properties of the superfluid in the dirty limit, where disorder interferes with the pairing mechanism. Disorder is conventionally introduced by immersing the liquid ^{3}He in silica aerogel.

The discussion has centered on the nature of the superfluid phases in this dirty limit [4–6]. The first evidence for a transition between different phases was found from NMR measurements [7]. Shortly thereafter, the magnetic phase diagram was measured over a wide temperature range [8]. The phase diagram at relatively low pressures is remarkably similar to that for the bulk phase, with an *A* phase in high magnetic fields and a *B* phase in low fields, separated by a first-order transition. This, along with several other measurements [6,7,9], provides strong evidence that the aerogel-confined phases are similar to their clean counterparts, and they are thus commonly designated the *A*-like phase and the *B*-like phase.

While NMR measurements provide convincing evidence that the *B*-like phase has the same overall structure as the clean *B* phase [6,10] (as has also been argued on theoretical grounds [11]), the nature of the *A*-like phase is still unresolved. Magnetic susceptibility measurements [5] show this phase to have the same susceptibility as the normal state, clearly implying that the *A*-like phase is an equal-spin pairing state. However, recent theoretical calculations suggest that the ABM state is not stable in aerogel and that the *A*-like phase should be quasi-isotropic and therefore unaffected by superfluid flow [11].

In the context of this controversy, we present here the first experimental observations of the mechanical properties of superfluid ^{3}He in aerogel. Our results provide strong evidence that the anisotropy in the *A*-like phase is very large and comparable to the ABM state. Furthermore, the order parameter of the *A*-like phase *must* give rise to a large anisotropy in the superfluid density.

To present the philosophy of the measurement, we note that the bulk *B* phase comprises an equal mixture of pairs with $\uparrow\uparrow$, $\downarrow\downarrow$, and $\uparrow\downarrow$ spin orientations with an energy gap which is isotropic in low magnetic fields. In contrast, the bulk *A* phase has only $\uparrow\uparrow$ and $\downarrow\downarrow$ spins pairs, yielding an anisotropic energy gap, with nodes along the orbital angular momentum axis $\boldsymbol{l}$. The $\boldsymbol{l}$ direction provides a long-range macroscopic directionality in the superfluid, yielding what is known as the "texture." Since the gap provides the effective "potential" experienced by the quasiparticle excitations, and is very different parallel to and perpendicular to $\boldsymbol{l}$, this direction (i.e., the orientation of the texture) has a very dramatic effect on the observed normal and superfluid densities.

The results below were obtained at the lowest accessible temperatures. We have investigated the anisotropy in two ways. From the effective transparency of the aerogel to oscillating superfluid flow, we can infer the superfluid density inside and how this varies with the flow velocity. By noting the damping of the motion, we can also probe the associated dissipation as a function of velocity.

The aerogels used consist of a dilute network of silica strands typically filling $\leq 2\%$ of the bulk volume, leaving $\geq 98\%$ of the volume available to the liquid ^{3}He. The strands are typically $\sim$3 nm across with a mean interstrand spacing of $\sim$20 nm. Measured quasiparticle mean free paths are around 100 nm for 98% aerogel [12] but with wide variation between samples [13,14]. Since the superfluid coherence length ($\sim$50 nm at low pressure, $\sim$15 nm at melting pressure [15]) spans this mean free path, the aerogel provides enough "impurity" scattering to suppress the superfluidity. For 98% aerogel, the suppression is complete at low pressures but only moderate ($\sim$20%) at high pressures.

The measurements are performed with a vibrating aerogel resonator similar to that of Ref. [8]. A 98% aerogel cylinder, 4 mm long and 2 mm in diameter, is glued to a 125 μm Ta wire, bent into the shape of a "goal post" as shown in Fig. 1. The resonator is mounted in the inner cell of a Lancaster-style nested nuclear demagnetization cooling stage [16]. The Ta wire is glued through the inner cell wall, and current and voltage twisted pair leads are attached in the outer cell. The inner cell also contains other vibrating wire resonators [17] for monitoring the cell temperature [18]. The cell is filled with ^{3}He and precooled in a 6.5 T field. Once demagnetized, the cell is able to reach ^{3}He base temperatures of around $0.1T_c^{\rm bulk}$ or $\sim$200 μK. All the measurements described here were performed at a pressure of approximately 16 bar.

We operate the aerogel resonator in a similar way to that for a conventional wire resonator [17]. An ac current is passed through the Ta wire. The Lorentz force produced in the vertical magnetic field provided by the demagnetization solenoid sets the wire and aerogel into oscillation. For this resonator, the vacuum frequency f_0 is 1167 Hz. The motion of the wire in the magnetic field generates a Faraday voltage proportional to the wire velocity. This voltage is amplified by a low-temperature transformer and measured with a lock-in amplifier.

We infer the superfluid density of the fluid in the aerogel from the resonant frequency of the resonator f, which is inversely proportional to the square root of the effective mass. The effective mass has three nontrivial contributions: (i) the mass of the resonator alone (inferred from the vacuum frequency f_0), (ii) the mass of the normal-fluid fraction entrained in the aerogel cylinder, and (iii) the effective mass of the fluid backflow around the cylinder. We note two conditions. First, the measurements are performed at temperatures so low that the surrounding bulk B-phase superfluid is essentially 100% superfluid. Second, the normal-fluid component inside the aerogel is clamped to the aerogel strands. Under these conditions, there are two obvious extremes. If the superfluid fraction in the aerogel were 100%, the aerogel would be completely transparent to the superfluid, it could move through the bulk liquid without displacing it, and there would be no backflow. The resulting resonant frequency would thus be close to the vacuum value. At the other extreme, when the fluid in the aerogel is completely normal and moves with it, the aerogel is completely opaque to the surrounding superfluid. The backflow around the cylinder is therefore at its maximum and the resulting resonant frequency at its minimum f_n. For an intermediate normal-fluid fraction inside the aerogel ρ_n, the effective mass of the confined ^{3}He and the superfluid backflow decrease proportionately. The superfluid fraction inside the aerogel phase $\rho_s/\rho = 1 - \rho_n/\rho$ is thus given by [8]

$$\rho_s/\rho = 1 - \frac{(f_0/f)^2 - 1}{(f_0/f_n)^2 - 1}, \quad (1)$$

where f_n is taken as 883 Hz as calculated from the high-T data.

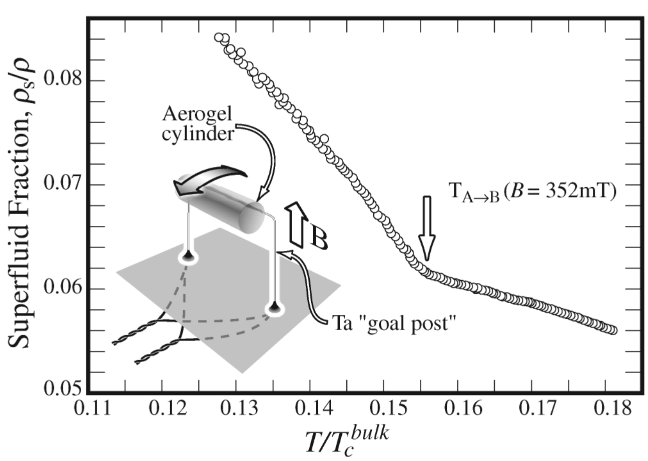

FIG. 1. The inferred superfluid fraction as a function of temperature, showing the A-B transition in aerogel. In the inset is shown the configuration of the aerogel resonator.

A typical low-velocity measurement of the superfluid density in the aerogel ρ_s/ρ as a function of temperature is shown in Fig. 1, taken as the cell is slowly demagnetized (cooled). Since the B-like phase is found to have a higher superfluid fraction than the A-like phase, the abrupt increase in the inferred superfluid fraction, observed at $0.156T_c$ and 352 mT, indicates the beginning of the A-like to B-like phase transition in the aerogel. As found previously [8], the transition does not show a discontinuous jump as one would expect for a first-order phase transition. This is due partly to the presence of a small magnetic field gradient across the sample and partly to pinning of the phase interface in the aerogel, which impedes an abrupt completion of the transition.

We now come to the crux of the experiment, the nonlinear behavior as the aerogel is driven to higher velocities. We observe simultaneously the superfluid fraction, ρ_s/ρ, and the damping of the motion as we ramp the velocity of the resonator by changing the drive level. [We take the damping force as the force per unit velocity at the resonant peak (in hertz) rather than the half-height frequency width, since the resonance is not strictly Lorentzian.]

The interesting behavior appears when we ramp up the velocity to some value, ramp it down again, then reramp it to successively higher velocities. The resultant observations for both phases are plotted in Figs. 2 and 3, which show the superfluid fraction and the damping, respectively. The behavior is quite remarkable. Referring to the A-like phase data in Fig. 2, as the velocity increases (A to B in the figure), the inferred superfluid fraction falls. When we stop and reduce the velocity (B to C), the superfluid fraction increases but at a significantly higher rate resulting in a higher superfluid fraction than was first observed. On subsequent sweeps, the behavior is quite reproducible but only if the velocity does not exceed any previous velocity. (Since the data are extremely temperature-dependent, the

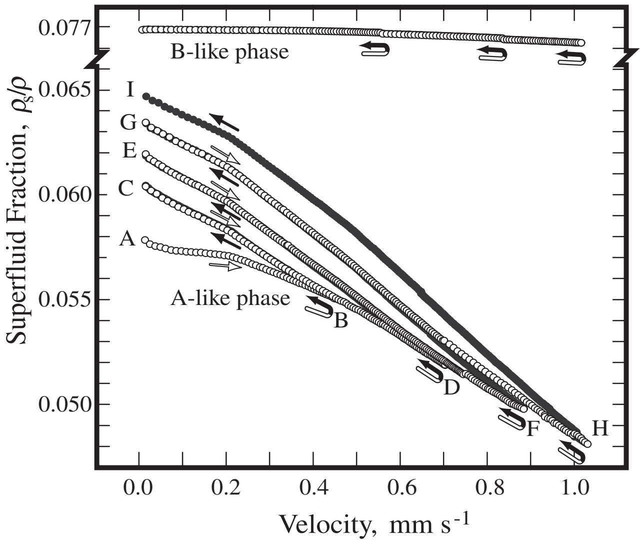

FIG. 2. The inferred superfluid fraction as a function of velocity at a temperature of $\sim 0.18 T_c^{\mathrm{bulk}}$. Open circles show sweeps with increasing velocity; solid circles show decreasing velocity. The upper data show the response in the *B*-like phase at a relatively low field (65 mT). The lower data show the response in the *A*-like phase (395 mT) with sweeps performed in order of increasing sweep range, *A* to *B* to *C* to *D*, etc.

very small mismatch between any downsweep and the next upsweep arises from the small power dissipated during the sweep which also limits the measurement to velocities below 1 mm/s.) The damping (Fig. 3) shows similar irreversible behavior, with a higher velocity-dependent damping corresponding to the higher superfluid fraction. The damping at the lowest velocities is reproducible and consistent with previous measurements [19].

The behavior of the *B*-like phase is entirely different. In Figs. 2 and 3, we show the corresponding behavior for the

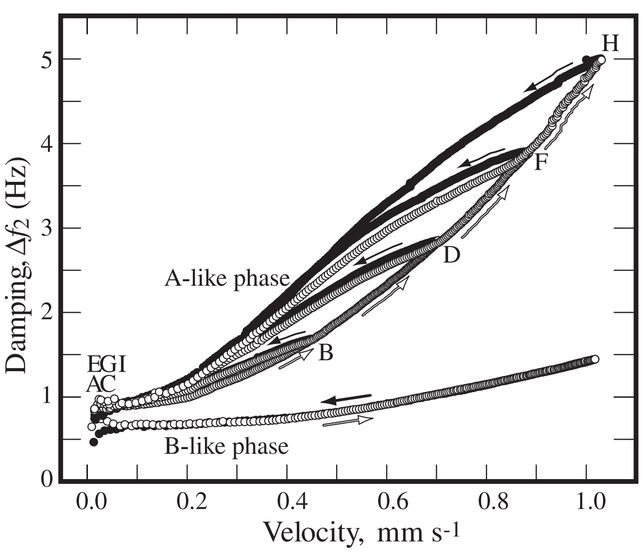

FIG. 3. The corresponding damping of the aerogel resonator as a function of velocity, for the data shown in Fig. 2.

B-like phase at a similar but slightly lower temperature. In Fig. 2, we see that the superfluid fraction is virtually independent of velocity and is so reproducible that upsweeps are indistinguishable from downsweeps. In Fig. 3, we see the same behavior for the damping in the *B*-like phase which, while increasing a little with velocity, is again entirely reproducible and nonhysteretic.

The *A*-like behavior is found to be insensitive to the magnetic field strength. We have also performed measurements partway through the *A*-like to *B*-like transition, where there is a mixture of phases. Here the hysteretic and nonlinear behavior decreases roughly in proportion to the fraction of the *A*-like phase present, confirming that the behavior is a property of the *A*-like phase alone.

That the *A*-like phase is clearly altered by an ac superfluid flow indicates that there must be significant anisotropy and associated textures. This is a very important result which helps identify the nature of the phase. There has been a difference of theoretical opinion on the possible order parameters of the superfluid phases in the presence of substantial impurity scattering [20,21]. While some recent NMR measurements [22] have been interpreted in terms of the *A*-like phase being associated with the ABM state [23], Fomin [11] has concluded that, in contrast to the clean *B* phase (BW state), the clean *A* phase (ABM state) should *not* be stable in aerogel. Furthermore, he argues that the allowed phases in aerogel, the so-called "robust" phases, have isotropic normal-fluid densities and, therefore, cannot be oriented by superfluid flow. This is clearly not what we see. However, Fomin's theory is strictly valid only in the Ginzburg-Landau regime and ignores magnetic scattering, whereas our measurements are performed at relatively low temperatures and high fields and the aerogel strands are covered with a magnetically active layer of solid ^{3}He.

It is useful to compare our findings with what might be expected if the *A*-like phase were closely related to the clean *A* phase (ABM state), which is highly anisotropic. The superfluid density is smaller parallel to $\boldsymbol{l}$ than perpendicular to $\boldsymbol{l}$. Consequently, superfluid flow tends to align the $\boldsymbol{l}$ texture along the flow axis, resulting in a lower superfluid fraction. The velocity scale for this change is set by the dipole velocity ~ 1 mm/s [24]. Our observations are semiquantitatively consistent with these properties. We can explain the velocity-dependent damping and irreversibility if we consider the pinning of textural defects that may occur in the *A* phase.

Our interpretation on this basis is shown schematically in Fig. 4. On cooling into the *A*-like phase, a rather scrambled $\boldsymbol{l}$ texture is first produced (state *A* in the figure) with many textural defects pinned by the aerogel. As the oscillation velocity increases, the flow begins to orient $\boldsymbol{l}$ along the flow direction (*B* in the figure), giving a reduced superfluid density and a consequent increase in damping. The superfluid flow through the aerogel will also tend to dislodge and expel or otherwise neutralize defects. This results in a more uniform texture which is maintained on the return sweep (*B* to *C*). The $\boldsymbol{l}$ texture prefers to align in

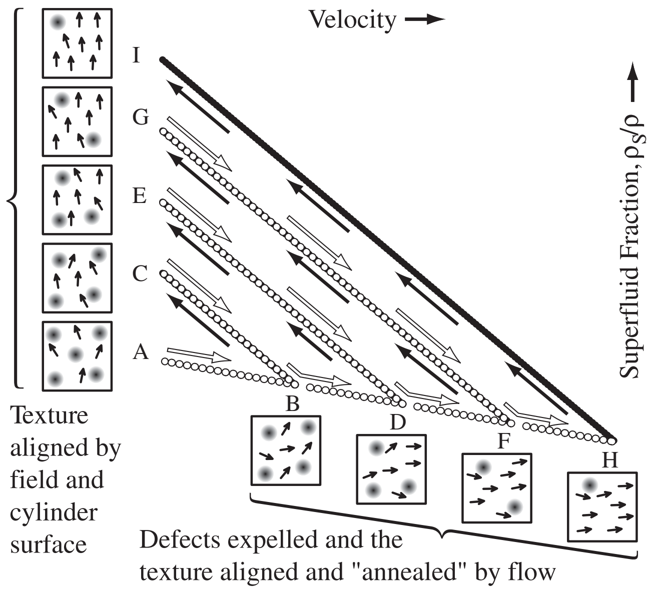

FIG. 4. Schematic interpretation of the data in Figs. 2 and 3. In the boxes, arrows show the ***l*** direction, and the spots show defect sites. Increasing the velocity expels defects, producing a more uniform texture. The flow velocity is perpendicular to the magnetic field. Thus, at low velocities, the fewer the defects, the better the texture aligns along the cylinder axis and the larger the measured superfluid fraction.

the plane of an *A*-*B* interface and perpendicular to a magnetic field. The surface of the aerogel represents an interface between the *A*-like phase and the surrounding clean *B* phase. The ground state of the ***l*** texture, at low flow velocities, will therefore be perpendicular to the field, in the plane of the aerogel surface, and therefore perpendicular to the flow direction, resulting in a higher inferred superfluid density. On increasing the velocity a second time (*C* to *B*), the behavior is reversible to *B* as the remaining defects are not depinned until the velocity exceeds the previous maximum velocity. At higher velocities, more defects become depinned and are washed away by the flow (*B* to *D*), resulting in an even higher superfluid fraction on the subsequent downsweep (*D* to *E*), and so forth. The equivalent points (*A*, *B*, *C*, etc.) are also marked in Figs. 2 and 3.

To conclude, we have presented here the first clear evidence that the *A*-like phase of superfluid ^{3}He in aerogel has a highly anisotropic normal-fluid density, in complete contrast to the *B*-like phase. We can modify significantly the *A*-like phase texture by applying a moderate superfluid flow through the sample. The flow orients the texture so as to produce a lower superfluid density along the flow direction. Our observations are qualitatively consistent with the *A*-like phase being very similar to the clean *A* phase. This runs counter to some of the recent theoretical investigations [11] which predict that disorder washes out anisotropy leading to a quasi-isotropic phases. Our findings have strong implications for the identification of the *A*-like phase in dirty superfluid ^{3}He and are consistent with a dirty ABM state.

We acknowledge financial support from the UK EPSRC under Grant No. GR/R54453, excellent technical support from I. E. Miller and M. G. Ward, and useful discussions with I. A. Fomin, H. E. Hall, and G. E. Volovik.

[1] R. Balian and N. R. Werthamer, Phys. Rev. **131**, 1553 (1963).
[2] P. W. Anderson and P. Morel, Phys. Rev. **123**, 1911 (1961).
[3] W. F. Brinkman and P. W. Anderson, Phys. Rev. A **8**, 2732 (1973).
[4] E. V. Thuneberg, S. K. Yip, M. Fogelström, and J. A. Sauls, Phys. Rev. Lett. **80**, 2861 (1998).
[5] D. T. Sprague, T. M. Haard, J. B. Kycia, M. R. Rand, Y. Lee, P. J. Hamot, and W. P. Halperin, Phys. Rev. Lett. **75**, 661 (1995).
[6] H. Alles, J. J. Kaplinsky, P. S. Wootton, J. D. Reppy, J. H. Naish, and J. R. Hook, Phys. Rev. Lett. **83**, 1367 (1999).
[7] B. I. Barker, Y. Lee, L. Polukhina, D. D. Osheroff, L. W. Hrubesh, and J. F. Poco, Phys. Rev. Lett. **85**, 2148 (2000).
[8] P. Brussaard, S. N. Fisher, A. M. Guénault, A. J. Hale, N. Mulders, and G. R. Pickett, Phys. Rev. Lett. **86**, 4580 (2001).
[9] G. Gervais, T. M. Haard, R. Nomura, N. Mulders, and W. P. Halperin, Phys. Rev. Lett. **87**, 035701 (2001).
[10] V. V. Dmitriev, V. V. Zavjalov, D. Ye. Zmeev, and N. Mulders, JETP Lett. **79**, 499 (2004).
[11] I. A. Fomin, J. Low Temp. Phys. **134**, 769 (2004).
[12] S. N. Fisher, A. M. Guénault, N. Mulders, and G. R. Pickett, Phys. Rev. Lett. **91**, 105303 (2003).
[13] P. A. Reeves, G. Tvalashvili, S. N. Fisher, A. M. Guénault, and G. R. Pickett, J. Low Temp. Phys. **129**, 185 (2002).
[14] S. N. Fisher, A. M. Guénault, A. J. Hale, and G. R. Pickett, J. Low Temp. Phys. **126**, 673 (2002).
[15] J. V. Porto and J. M. Parpia, Phys. Rev. Lett. **74**, 4667 (1995).
[16] G. R. Pickett and S. N. Fisher, Physica (Amsterdam) **329B–333B**, 75 (2003).
[17] A. M. Guénault, V. Keith, C. J. Kennedy, S. G. Mussett, and G. R. Pickett, J. Low Temp. Phys. **62**, 511 (1986).
[18] C. Bäuerle, Yu. M. Bunkov, S. N. Fisher, and H. Godfrin, Phys. Rev. B **57**, 14 381 (1998).
[19] D. I. Bradley, S. N. Fisher, A. M. Guénault, C. J. Matthews, P. Skyba, G. R. Pickett, and K. L. Zaki, J. Low Temp. Phys. **138**, 123 (2005).
[20] G. E. Volovik, JETP Lett. **81**, 647 (2005).
[21] V. P. Mineev and M. E. Zhitomirsky, JETP Lett. **81**, 296 (2005).
[22] V. V. Dmitriev, I. V. Levitin, N. Mulders, and D. Ye. Zmeev, JETP Lett. **84**, 461 (2006).
[23] G. E. Volovik, JETP Lett. **84**, 455 (2006).
[24] D. Vollhardt and P. Wölfle, *The Superfluid Phases of Helium 3* (Taylor & Francis, London, 1990).